Study of prevalent background for the eBubble-low energy solar neutrino experiment

Sarah Lewin

Columbia University-Nevis Laboratories, Irvington, New York

Abstract

The eBubble collaboration is motivated by the thirst for knowledge on the topic of what processes fuel our sun. Specifically, the project is plans to detect the solar neutrinos that are the products of proton-proton fusion. This solar reaction produces the highest flux of electron neutrinos, and yet this source of solar neutrinos has remained unexplored due to its inherently weak signal (low rate and small energy). eBubble will be the a detector sensitive to both the spectrum and the rate of these elusive neutrinos. The research documented here will address the pressing background issues that haunt experiments working with a signal of such a low rate (0.001 per day per kg of Neon) and such a low energy. This study has shown, as hypothesized, that the main background for WIMP detectors, produced by the neutron byproducts of radioactive impurities in the detector itself, is of negligible concern. The more pressing background issue comes from a much higher background signal produced by photon compton interactions. This will also be discussed.

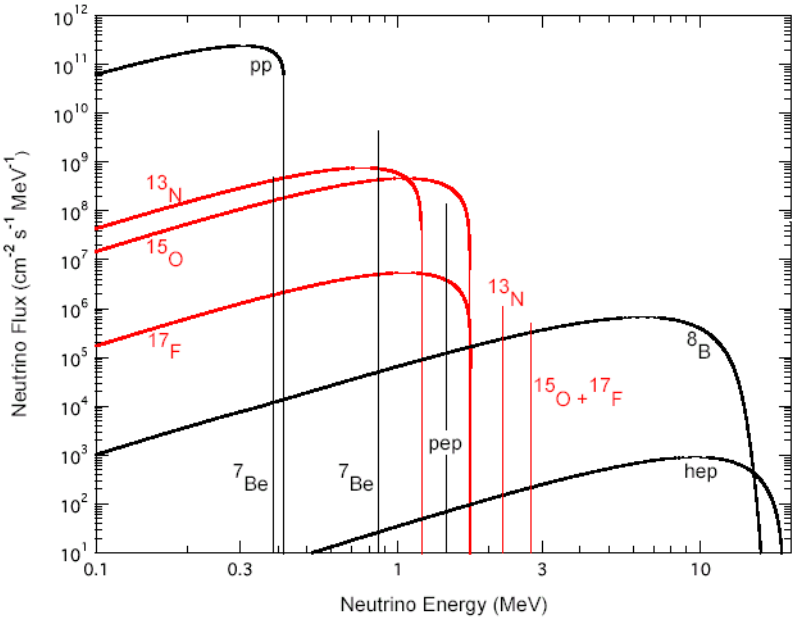

FIG. 1: The proton proton fusion reaction in the sun produces the highest flux of solar neutrinos.[1]

I. INTRODUCTION

A. Why Study Low Energy Solar Neutrinos?

Although the eBubble concept envelopes many opportunities to discover new physics, it is being presented foremost as a tool to study the low-energy solar neutrinos, in the hopes of further exploring the standard solar model. The project's capabilities include, but are not limited to: studying the energy spectrum of solar neutrinos with high precision, studying the neutrino oscillation phenomena, and probing the innermost workings of the sun. The neutrino physics questions that can potentially be answered by these new tracking technologies are numerous.

B. eBubble's Plan

The eBubble project proposes a new tracking detector to probe p-p fusion reactions in Sun. The reaction involves the fusion of two hydrogen nuclei into a deuterium nuclei (one proton and one neutron), and produces a positron and electron neutrino. While this reaction produces the highest flux of solar neutrinos, their characteristic energy has been, until now, too low to measure experimentally by standard measures.

eBubble boasts the birth of a new concept: cryogenic noble fluids in tracking detectors through the controlled transport of electron bubbles. The three cryogenic fluids: Helium, Neon, and most recently Hydrogen display a shared characteristic: the encapsulation of free injected electrons by a vacuum filled "bubble" with a diameter on the order one nanometer[2]. This phenomena is a result of both a very strong Pauli repulsion between the injected electron and the noble atoms, and a lack of polarizability of Helium and Neon that is present in the heavier noble elements.

These electron bubbles have more than one useful characteristic of which the detector intends to take full advantage of. The extended size of the electron bubble serves to greatly decrease mobility and aids in the detecting instrumentation for track imaging.

C. Detector Construction

The proposed construction for a meter cubed proof of concept prototype is detailed in Figure 2. The detector, as well as my simulation, most importantly consists of three materials. Our target fluid, the cryogenic noble neon, will be doped with 0.1 percent hydrogen, for gain purposes which hold little bearing on my background concentrated research. The cryogen will be contained inside a pure copper liner 8 inches thick, which will itself be contained in 1.5 inches of stainless steel. These three components, as will be discussed later, were those used in producing a simulation of the background signal that my research was committed to analyzing.

D. Our Signal

The eBubble detector will measure the convolution of the neutrino flux spectrum and the electron scattering partition. Figure 3 depicts the probability of producing electrons with different recoil kinetic energies as a function of the kinetic energy itself. Tracking detectors thus far have lacked the sensitivity to dip into this realm of the neutrino energy spectrum produced by the proton-proton fusion. One can see that it is most probable for the neutrino to deposit very little energy onto our target electrons. From this anticipation it follows that the signal is expected to occur at an exceptionally low rate, roughly 0.001 events per day. It is thanks to this weak signal that a more careful analysis of potential background sources

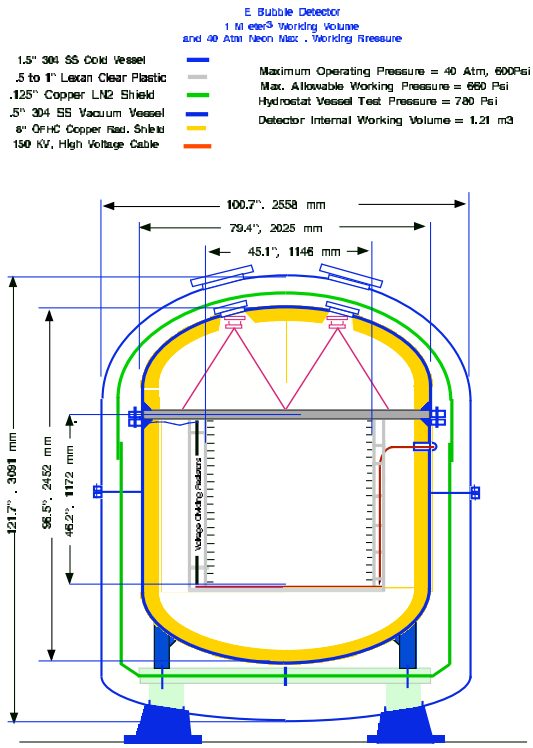

FIG. 2: The schematics of our meter cubed proof of concept prototype.

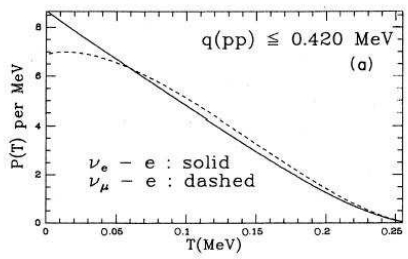

FIG. 3: This plot shows the standard solar model's predicted probability of an incident neutrino producing electrons with different recoil kinetic energies as a function of the scattered electron kinetic energy. The signal peaks at zero, and falls off near 0.25MeV.[1]

is necessary.

E. The Background on Background

There exists an extensive list of low energy detector experiments that are required to take similar background related precautions. These experiments must evaluate the following:

The earth's atmosphere is incessantly bombarded by cosmic radiation. The most effective

way to reduce the incoming cosmic ray background is to place the experiment underground. Depending on the depth below the earth's surface, this muon induced background can be acutely attenuated. A possible location for the eBubble prototype is the Homestake Mine. The decommissioned underground gold mine in South Dakota was chosen by the NSF as the site for DUSEL (Deep Underground Science and Engineering Laboratory).

Natural radioactivity presents perhaps the most oppressive component of background. Naturally occuring radioactive impurities in the immediate environment of the detector can be effectively minimized by shielding. However, that still leaves the radioactive impurities of the shields themselves. Careful selection of the detector component materials to minimize radioactive impurity levels is the only solution.

F. Pure Materials

As previously discussed, the three components of our detector that are critical to an accurate simulation of the background are stainless steel, copper, and our neon cryogen.

The cryogenic noble fluid, neon, not only boasts the unusual characteristic of electron bubble creation, but also is an inherently pure material with no natural radioactive isotopes. By nature of liquid neon's boiling point, 27 degrees Kelvin, any impurities will "freeze out" to the walls of the detector so as not to contaminate our intrumented target volume.

The copper used in the 8 inch copper lining of the detector can very easily be attained with a purity level orders of magnitude greater than the stainless steel, which presents perhaps the most significant component of radioactive background.

Thus even providing our detector with the purest available materials, an irreducible level of background is inescapable.

1. Radioactive Impurities in Stainless Steel

The remaining background, that whose analysis this documentation is dedicated to, will be produced by the radioactive isotopes present in stainless steel. The most common isotopes are thorium 232, uranium 235 and uranium 238. These isotopes have radioactive decay chains known to produce an abundance of alpha and beta particles, as well as gamma emissions.

Once again, my motivation has been to confirm the hypothesis that the neutron induced background that burdens WIMP detector experiments will not be a pressing issue for the eBubble project. In fact a photon spectra should demand most of our attention.

The alpha and beta particles themselves that are emitted when an unstable isotope radioactively decays to a more stable one are massive. An alpha particle has an atomic number of two and an atomic mass number of four, meaning the particle containts two protons and two neutrons. Beta particles consist of electron, positron, and nuetrino combinations. Thus they have very little range and are unlikely to penetrate into our target fluid.

However, the gamma emissions, which occurs when an excited nucleus emits a high energy photons, are neutral and massless, and produce a signal in our target fluid that is nearly indiscernible from the desired neutrino signal.

II. PHOTON BACKGROUND DUE TO COMPTON SCATTERING

When an excited nucleus decays to a more stable state, it radiates a photon. This is a frequent occurence over the course of a radioactive isotopes decay chain. Should this photon enter into our target fluid, interact with a target electron, depositing a small enough amount of energy, and then escape further detection in our fluid, it may be absolutely indistinguishable from our neutrino signal. However, careful consideration of these compton scatterings reveals that photons may present less of a problem than initially conjectured. If the entering photon is a high energy one, which deposits most of its energy (more than 250keV) in one interaction, and then escapes, we can identify this interaction as background and remove it. Our signal (see Figure 3) is hypothesized to fall off past 0.25 MeV [3]. It is more likely, however, that a high energy photon will deposit small amounts of energy during several well separated Compton interactions, in which case these interactions can be identified as background (since the neutrino signal consists of one low energy interaction) and removed. Finally, should a low energy photons be emitted from the radioactive decays chains in the stainless steel, it would have very low penetration depths, and it is improbable that they would make it through the rest of the 1.5 inches of SS and 8 inches of Copper.

Though the probability seems low, gamma emission was by no means eliminated from the very thorough analysis of potential background. Specifically, our my research concentrated on a 2.614 MeV photon, which is known to radiate from thallium 208 35.6 percent of the

time a parent thorium 232 isotope decays[4].

A. Photon Simulation

TABLE I: Final results for the a generated N-Tuple with one million photon events are displayed. The two cuts of interest include an energy cut requiring interactions to have an energy of less than 250keV, and a fiducial volume cut which put upper and lower bounds on the Z component of the interactions. These results are the number of events/day/kg of fluid neon of the radial slice, for a stainless steel with 0.6 ppb of thorium 232. Also shown is the effect of decreasing the radial instrumentation from 100cm to 50 cm.

isotope	no cuts (50cm/100cm)	with z cut (50cm/100cm)	with z and energy cuts (50cm/100cm)
th232	20341/52229	9066/26190	5258/10023

For my research, I used a geant simulation provided to me, which simulates the interactions of particles with incident matter. The simulation consists fundamentally of the construction of the detector and the generation of the primary events. The detector construction my results are based on consists only of the 1.5 inches of stainless steel shield, with the cryogenic neon as our target. The dimensions are consistent with those seen in Figure 2. The photon "events" are randomly generated throughout the stainless steel with a fixed energy of 2.614 MeV.

B. Photon Results

For my analysis, one million photon events were generated with the energy of 2.614 MeV for the aforementioned motivations. Each event was given a weight of 0.03, which represents how many photons per day are expected for our 426.9 kg mass of stainless steel containing 0.6 parts per billion of thorium 232 radioactive isotope impurities. A basic code then sliced our cylindrical detector into 10 centimeter thick radial slices out to 1 meter. The resulting histograms depict how many events with only one interaction occur in each radial slice. It is these events that interest us, since our neutrino signal will be composed of events with only one interaction with our target fluid. Several cuts were implemented to reflect both the effects of the realistic fiducial volume of our 1 meter cubed prototype, as well as the

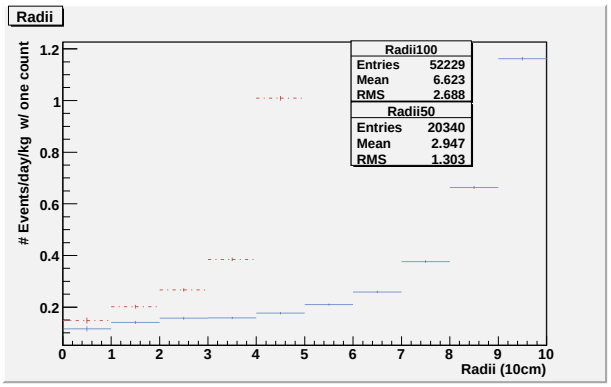

FIG. 4: One million photon events were generated. Events with only one interaction are binned in this histogram according to which 10 centimeter radial slice the interaction occurs in.

possible effects of being able to only instrument our detector radially out to 50 centimeters as opposed to the full meter.Potentially reducing the instrumentation, hypothetically due to budget complications, would most notably increase the background for the radial slice between 40 and 50 centimeters. This discrepancy becomes minimal toward the more central slices.

Keeping in mind that the neutrino signal will occur at a rate of 0.001 events/day/kg of Neon, the background noise from photons eliminates the validity of the signal much past the inner radius of 20 cm. It is important here to note that the implementation of the 8 inches of pure copper liner will decrease our photon background by at least an order of magnitude, as evidenced by the previous year's results. Also, increasing the detector's volume urther decrease the irreducible background in the center of the detector , as the background would follow the same drop off trend displayed in all of the histograms.

III. NEUTRON BACKGROUND

Once again, lets not forget the concentration of this research: the analysis of the background eBubble is presented with, specifically to confirm that the neutron background that burdens experiments probing WIMPS are not an issue for our low energy solar neutrino detector.

The two sources of neutron background simulated, are both results of the radioactive decay of isotope impurities in the stainless steel shield: alpha-neutron reactions and spon-

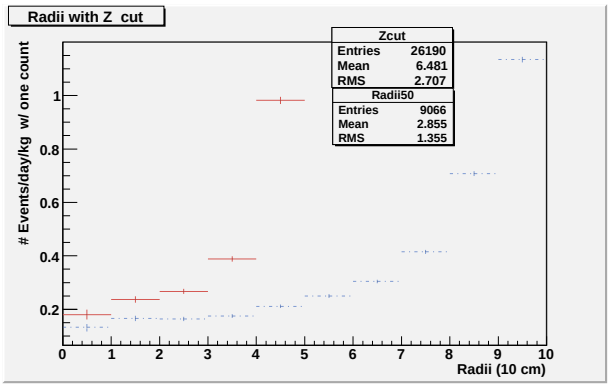

FIG. 5: One million photon N-tuple, with the fiducial volume cut that excludes interactions whose Z component is not within the requirement: $-391mm < Z < 580mm$.

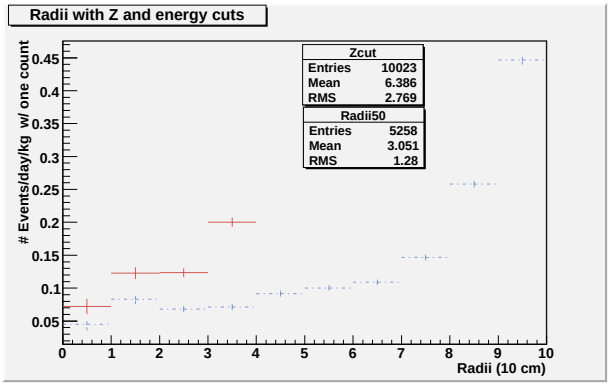

FIG. 6: The same N-tuple with one million photon events, with the energy cut that excludes interactions with a kinetic energy of over 250keV and the fiducial cut that excludes any interactions whose z position in the detector is outside of the fiducial volume, whose measurements can be seen in the the schematic in Figure 2.

taneous fission.

While the alpha particles that are emitted during radioactive decay chains are not themselves an issue, due to their weak penetration strength, the alpha particles DO collide with other components of the stainless steel, and are thus a catalyst for atoms emitting neutrons. These neutrons, being neutral, and having a much smaller mass than the alpha particles themselves, are more than capable of penetrating into our target neon fluid, and interacting with an electron just as a neutrino would...thus producing a potentially indistinguishable background from our signal.

Another source of neutron background is the spontaneous fission of radioactive isotopes.

Spontaneous fission follows the exact same process as nuclear fission, except that it occurs without the atom having been struck by a neutron, or an alpha, or any other incident particle. A radioactive nucleus disintegrates into two or more smaller nuclei and other particles, such as neutrons that, again, can also interact with a target electron and produce a background signal.

A. Neutron Simulation

The process of simulating the background produced by neutron interactions was a bit more complicated than that of simulating photons. Rather than generating neutrons of one energy, a more thorough analysis required an energy spectrum comparable to what we believe will occur experimentally. Courtesy of the Xenon project collaboration, we were provided with generated data from a SOURCES simulation, which produced several useful neutron energy spectra. The data provided a probability of neutron flux (neutrons/second-cm cubed), as a function of energy in MeV. Four separate data files were provided. Two of the files contain spectral data for a stainless steel consisting of : C 0.15%, Cr 17%, Ni 12%, Mn 29%, and Fe 68.85%. The other two files contain spectrail data for another stainless steel: Fe54 88%, Co59 8%, and C54 4%. For each of these two types of stainless steel, there are two seperate sets of spectral data. One file for each of the different stainless steel components provides the data for a hypothetical impurity level of 10 ppb of thorium 232, while the other provides data for uranium impurities of: 9.928 ppb U238 and 0.072 ppb U235.

The event generator of the neutron simulation would sample the neutron flux from these spectra in order to determine the probabilities of a neutron event with certain energies. A first check of our simulation was simply confirming that the generated neutron spectrum used as an input was within statistical fluctuations of the simulation's output spectra.

IV. NEUTRON RESULTS

For the neutron background analysis 10,000 events were generated, and the same process was followed as for the photons, with the exception of the defined weight for each of the four neutron files. The weights can be seen in Table III.

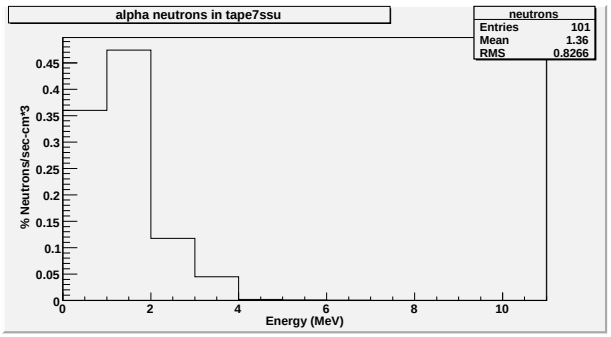

FIG. 7: The sources simulation provided spectral data for alpha particles acting on separate components of the stainless steel, as well as a total spectrum for all alpha-neutron reactions, which is seen here.

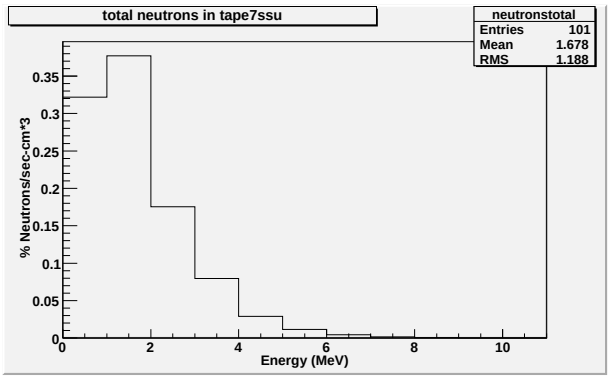

FIG. 8: The spontaneous fission neutron spectrum and the alpha-neutron spectrum combined to create a total neutron spectrum.

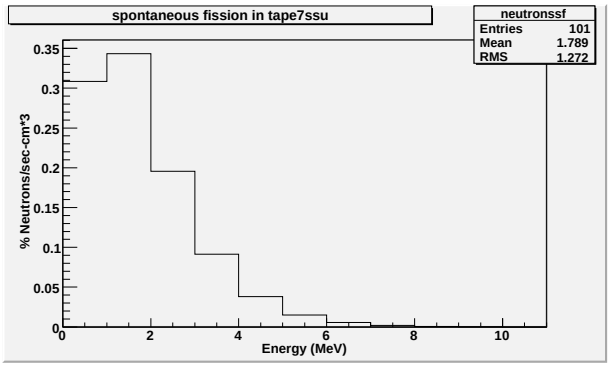

FIG. 9: The sources simulation also provided a total neutron energy spectrum for spontaneous fission reactions.

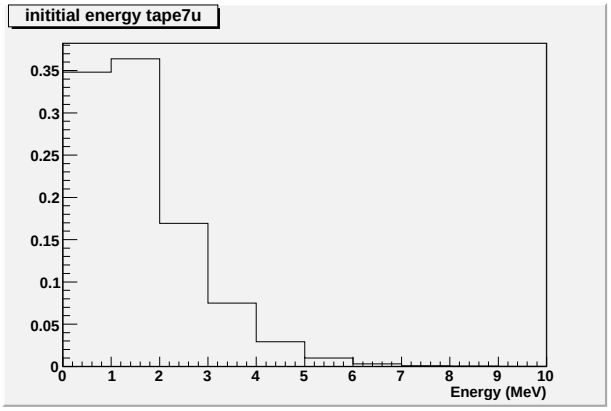

FIG. 10: A simple check of the simulation is to make sure that the generator is correctly sampling the input data to produce neutrons with initial energy within statistical errors of the input spectrum.

TABLE II: The weight of each event was simply calculated by multiplying the total neutron flux (neutrons/s-cm cubed) by the volume of the neon fluid (852,379.2 cm cubed) times the appropriate time unit conversion, to give us a final unit of events/day/kg of Neon. Again, the units displayed in the histograms are divided by the weight in kilograms of the individual radial slice in which the interaction took place.

ss with isotope	# of neutrons/day
ss th	11
ss u	87.5
tape7 u	107.5
tape7 th	36.1

The same basic code then sliced our cylindrical detector into 10 centimeter thick radial slices out to 1 meter, just as before. The resulting histograms depict how many events with only one interaction occur in each radial slice. Identical instrumentation, fiducial volume, and energy cuts were implemented. Table II displays the final numbers: total events with one interaction within 50 centimeters as well as out to the full meter of the chamber for both the "Z-cut" as well as the energy cut. With this final energy cut, the rate of neutron interactions that are indiscernible hovers below the expected neutrino signal of approximately 0.001 interactions/day. The number of these neutron interactions will be

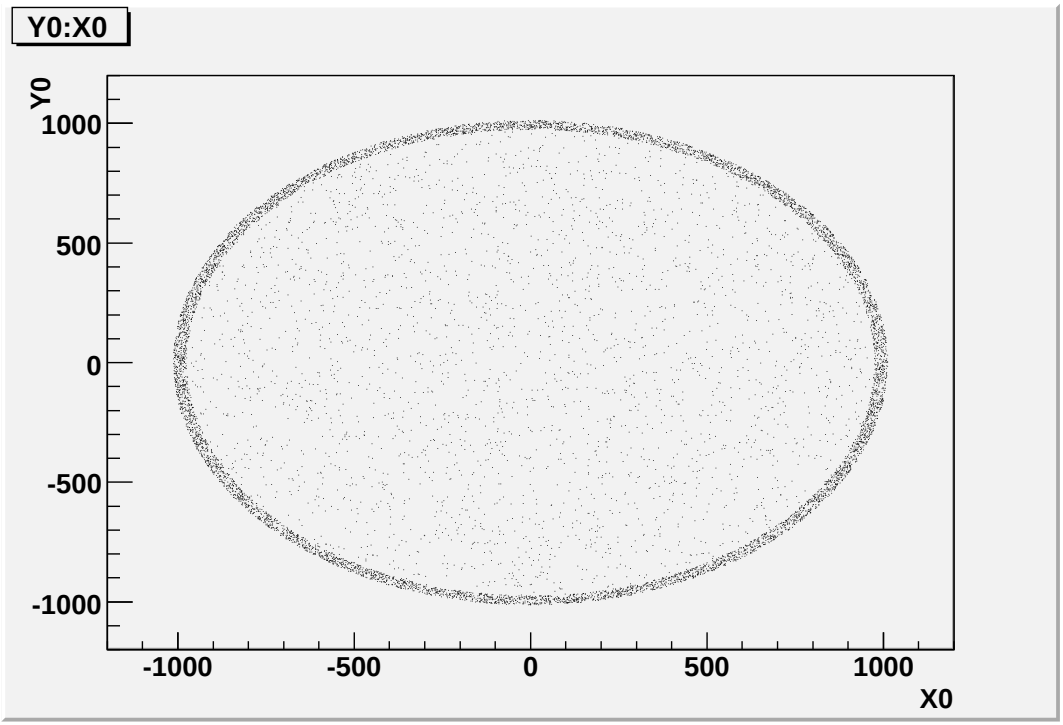

FIG. 11: Events are randomly generated throughout the inner lining of the cylindrical vessel. This plot shows the initial x and y positions of the events produced by the primary generator. The events seen in the center of the image are those that are generated in the caps of the cylinder.

further attenuated by the pure copper lining, as well as the decrease in impurity levels, from around 10 ppb to less than one ppb, for the stainless steel that will realistically be used to construct our detector.

V. CONCLUSION AND FUTURE WORK

The results of this research have successfully confirmed the hypothesis that the neutron background would prove to be an almost negilible source of background noise in the eBubble noble fluid tracking detector. The improvements to follow will constitute a significant decrease in the backgrounds documented here. Again, the realistic levels of impurity for stainless steel will be at least an order of magnitude less. Also, the 8 inches of pure copper that will be placed inside the cold vessel steel wall, will greatly reduce the background coming from the SS impurities. However, the exact components and impurity levels of our stainless steel, as well as the copper lining need to be accurately implemented in our simula-

TABLE III: Final results for the four neutron energy spectral data. The two cuts of interest include an energy cut requiring interactions to have an energy of less than 250keV, and a fiducial volume cut which put upper and lower bounds on the z component of the interaction. The numbers seen are in number of events.

type of stainless steel and isotope impurity	no cuts (50cm/100cm)	with z cut (50cm/100cm)	with z and energy cuts (50cm/100cm)
tape7 th	256/1483	75/539	22/199
tape7 u	260/1487	72/546	28/175
ss th	329/1515	85/543	38/144
ssu u	296/1511	65/574	18/184

tion for more realistic results. Finally, as with all low energy detectors, potential scalability, in essence an increased volume, is always considered an improvement. As the target fluid itself serves as a shield to unwanted background interactions, the level of noise drops off almost exponentially toward the center of the detector. Thus, the greater the volume, the greater the sensitivity neutrino signal.

VI. SPECIAL THANKS

I would like to extend a gracious note of appreciation for the support and guidance I've received over the course of the program from Dr. Raphael Galea and Professor Jeremy Dodd. Also thanks to Nevis Labs and Columbia University, as well as John Parsons and William Willis, responsible each in part for my participation this summer.

---

[1] J. Bahcall and C. Pena-Garay, New J. Phys. 6, 1 (2004).

[2] C. Kuper, Phys. Rev. 122, 1007 (1961).

[3] J. Adams, Y. Huang, Y. Kim, R. Lanou, H. Maris, and G. Seidel, in Low energy solar neutrino detection (World Scientific Publishing, 2001), p. 70.

[4] `http://hepwww.rl.ac.uk/ukdmc/Radioactivity/Th_chain/Th_chain.html`

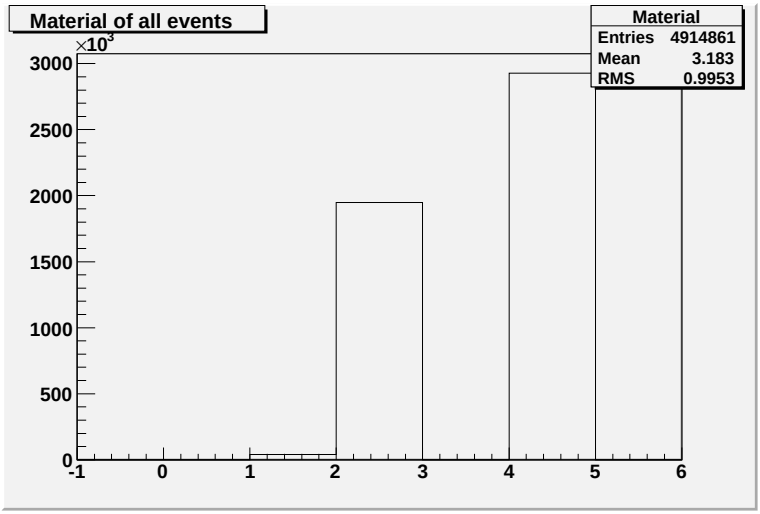

FIG. 12: The material in which each interaction took place: 0=initialized state, 1=air, 2=gas, 3=CuBe Wall (not implemented), 4=SS Wall, 5=Cu Liner (also not implemented).

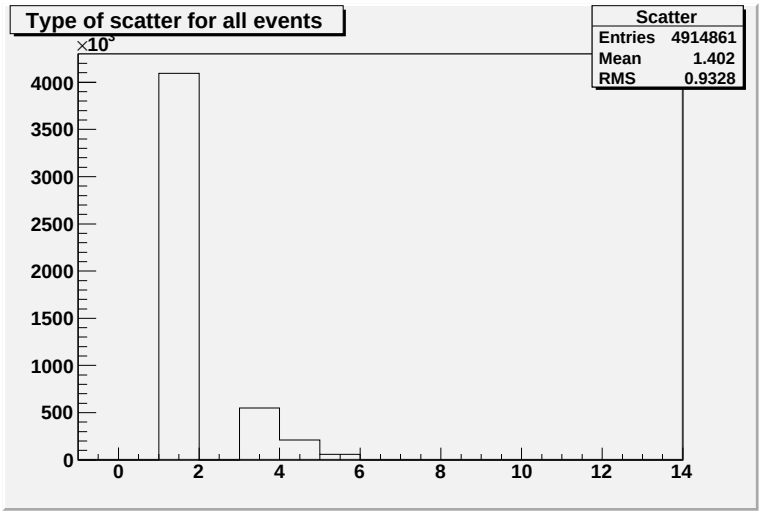

FIG. 13: This histogram designates what type of scatter each interactioni was. 0=initialized state,1=Compton,2=other Geant ionization, 3=photoelectric effect, 4=Rayleigh,5=Conversion.

VII. APPENDIX

A. Photon histograms

B. Neutron Histograms

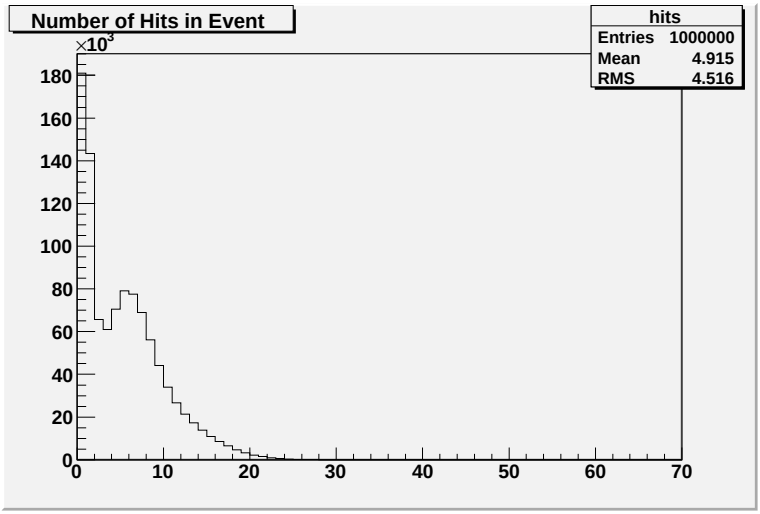

FIG. 14: Number of interactions in each event.

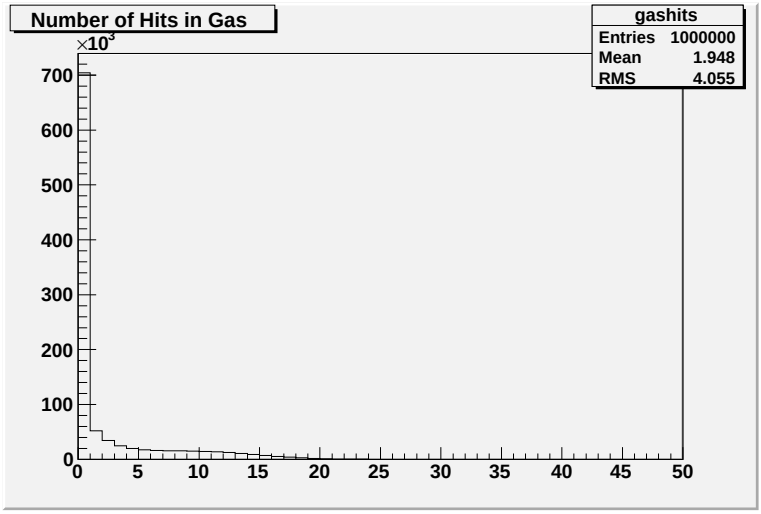

FIG. 15: Number of interactions for each event in the gas.

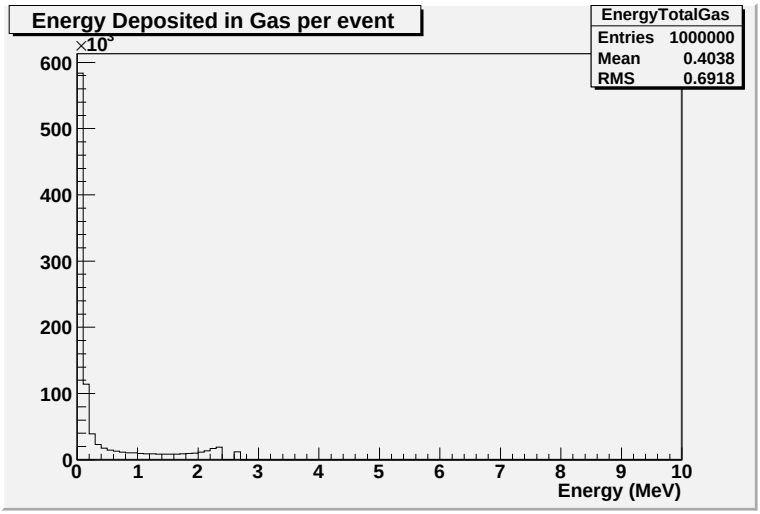

FIG. 16: The amount of energy deposited in the target Neon per event.

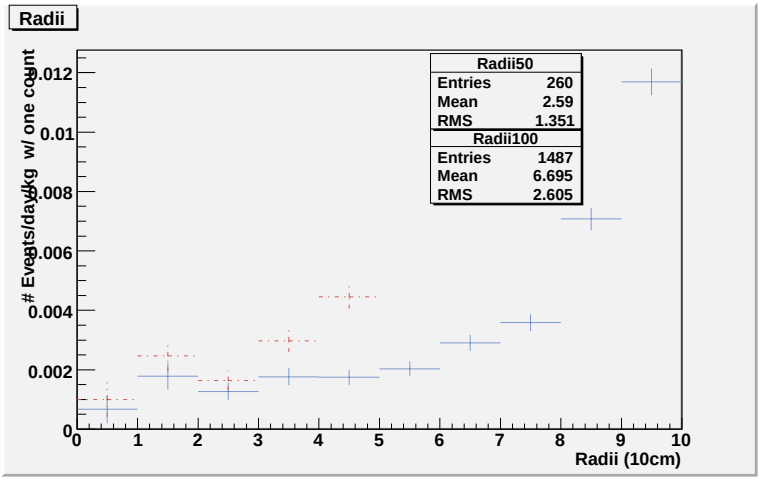

FIG. 17: tape7 U

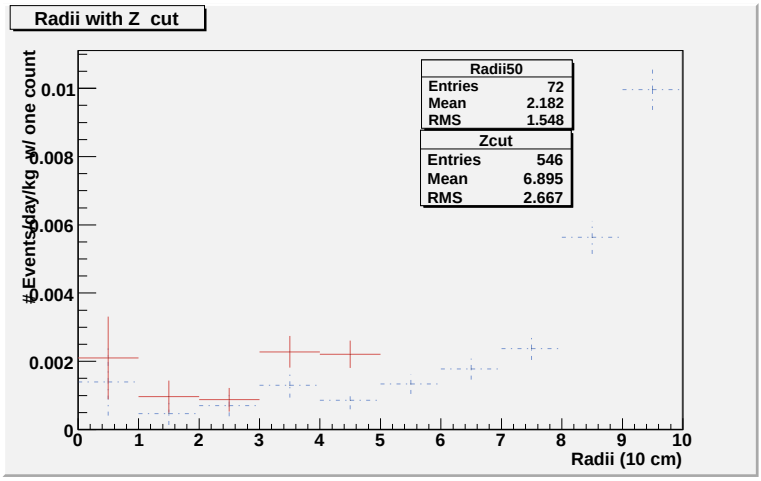

FIG. 18: tape7 U

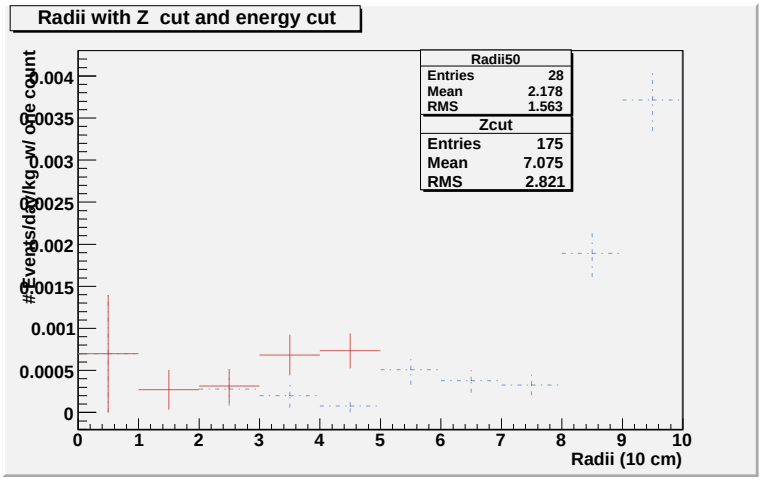

FIG. 19: tape7 U

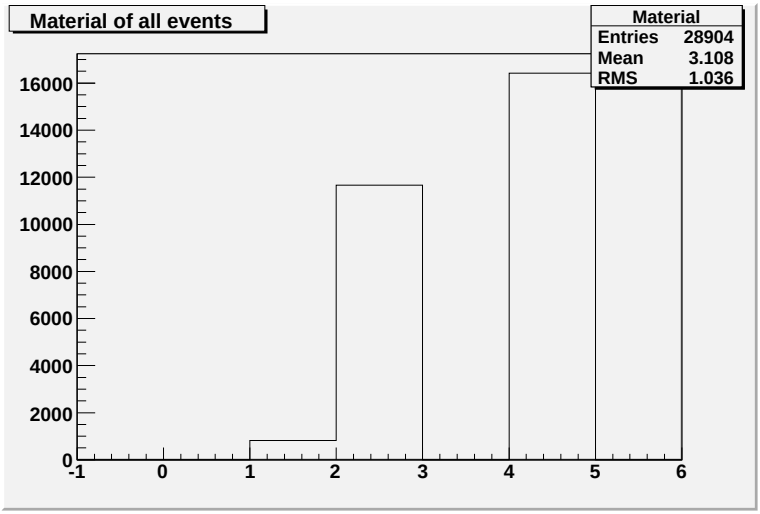

FIG. 20: tape7 U

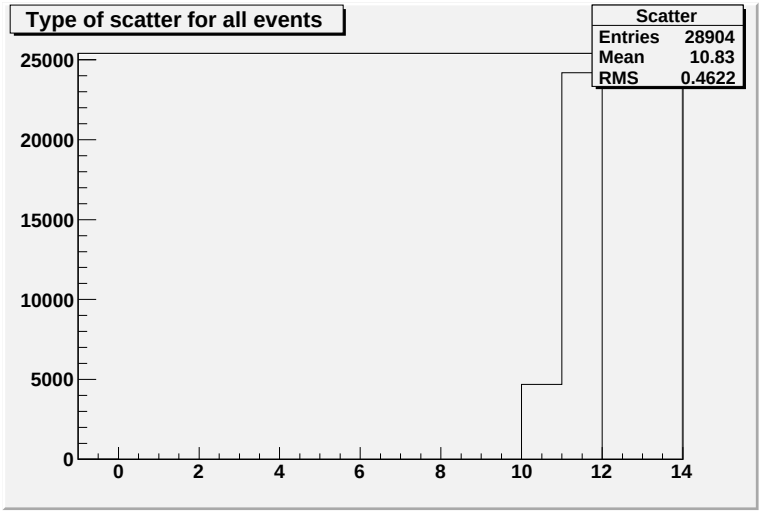

FIG. 21: tape7 U

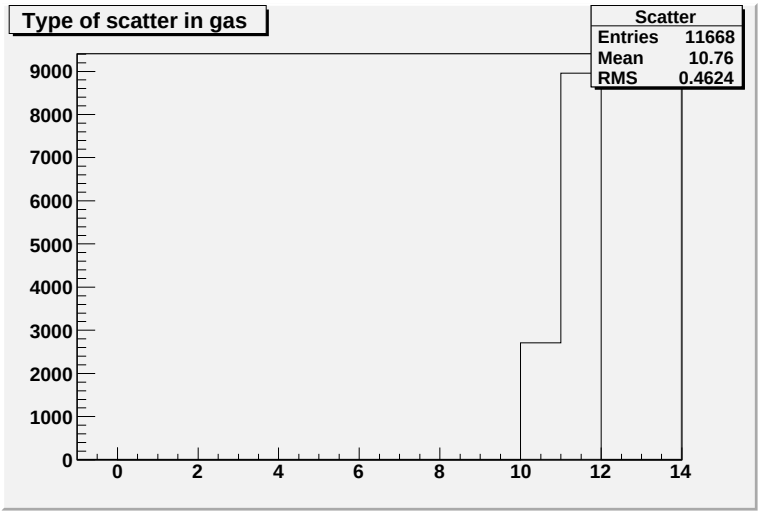

FIG. 22: tape7 U

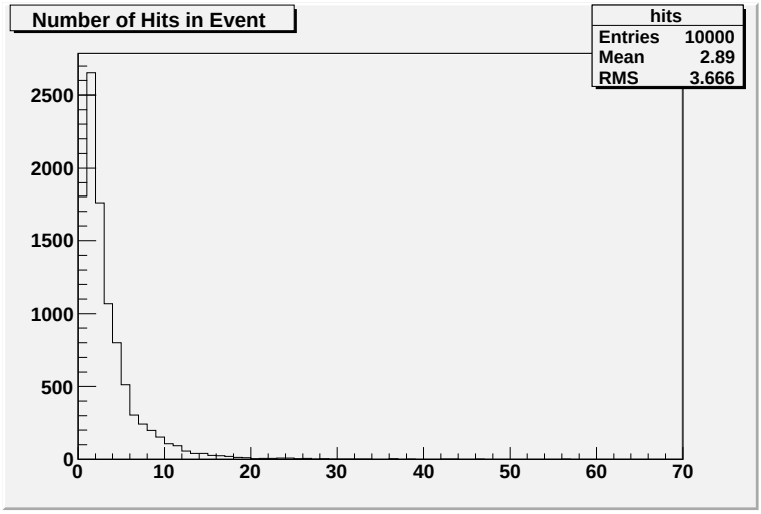

FIG. 23: tape7 U

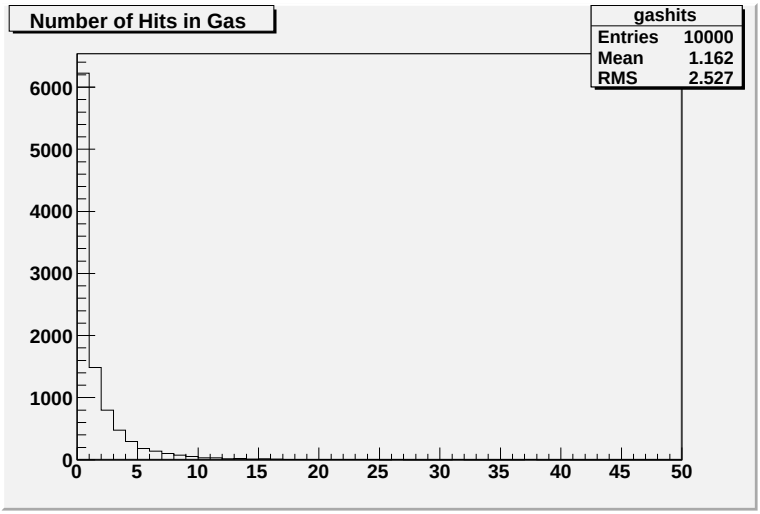

FIG. 24: tape7 U

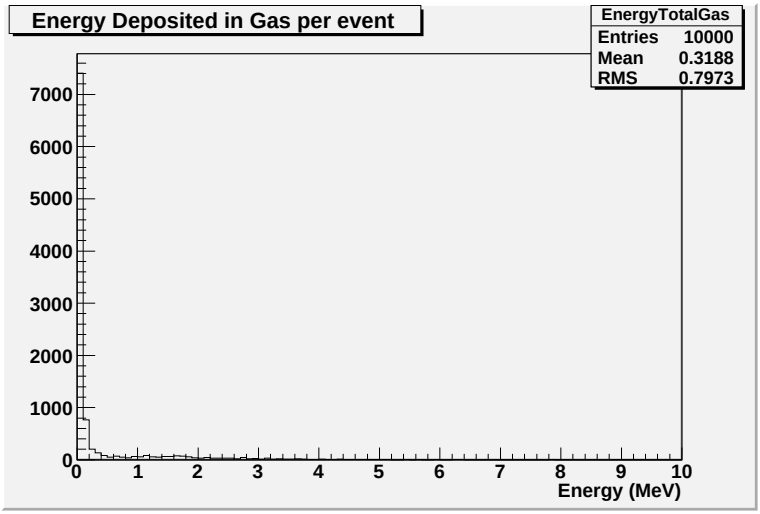

FIG. 25: tape7 U

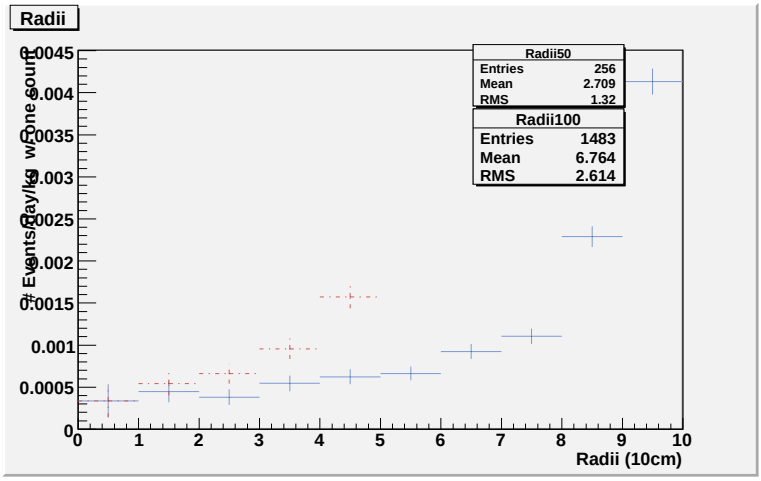

FIG. 26: tape7 th

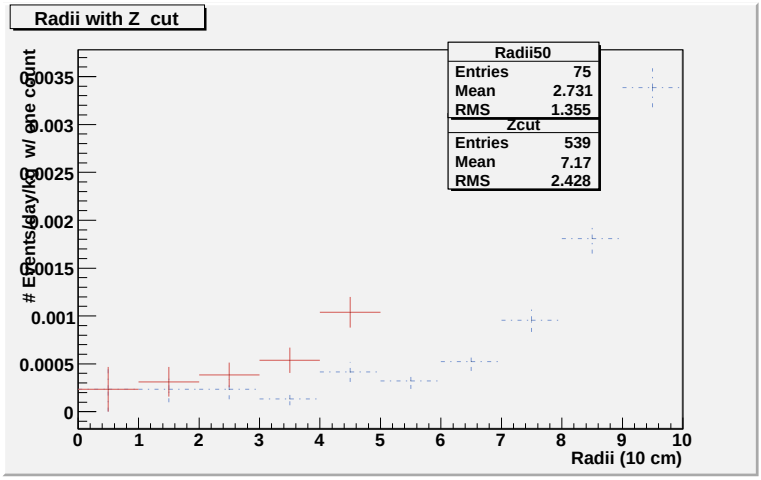

FIG. 27: tape7 th

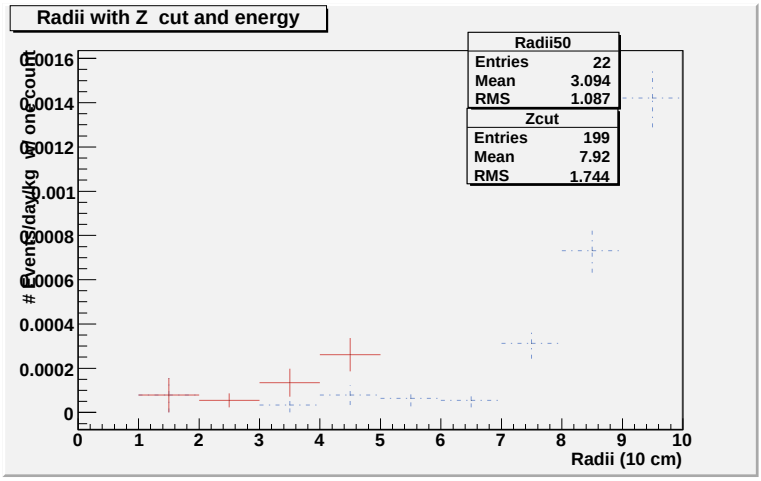

FIG. 28: tape7 th

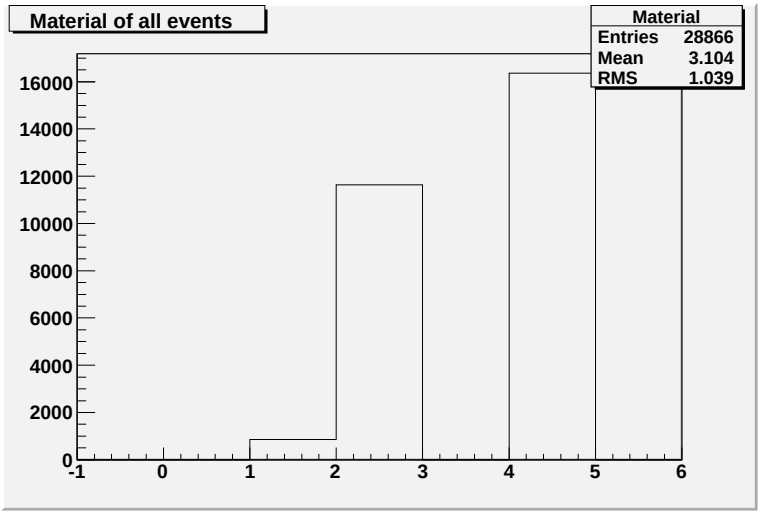

FIG. 29: tape7 th

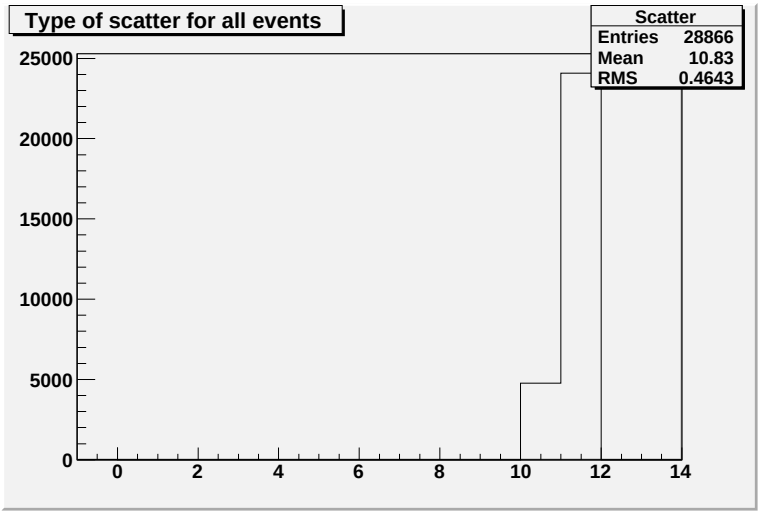

FIG. 30: tape7 th

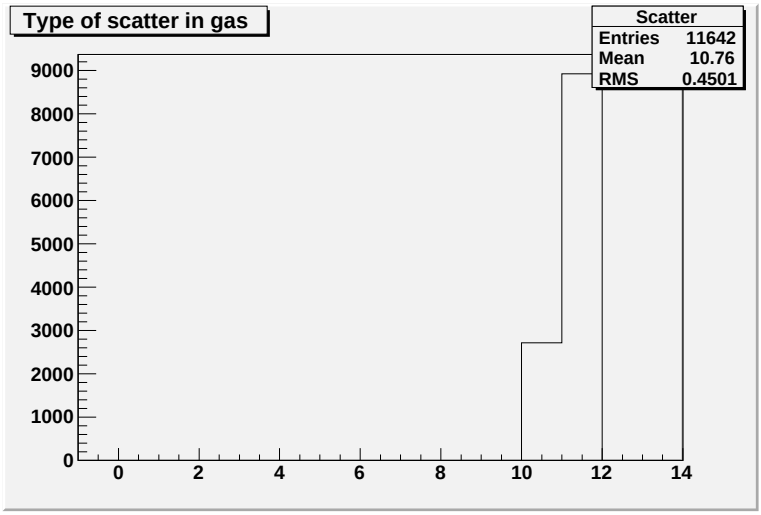

FIG. 31: tape7 th

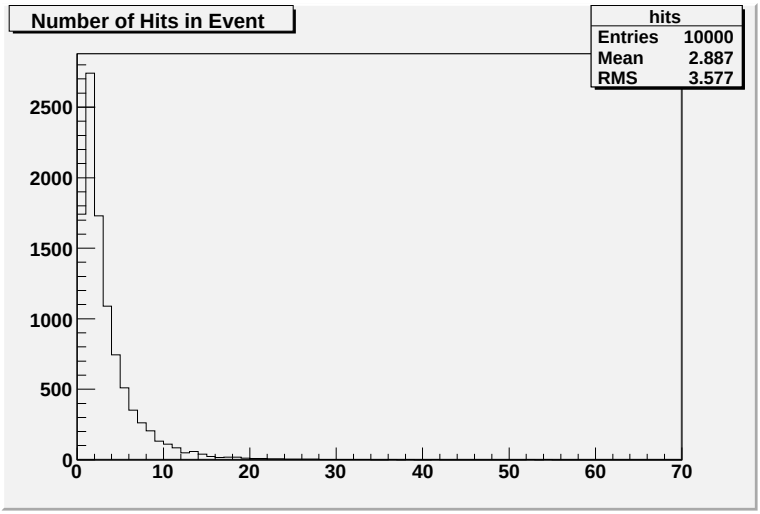

FIG. 32: tape7 th

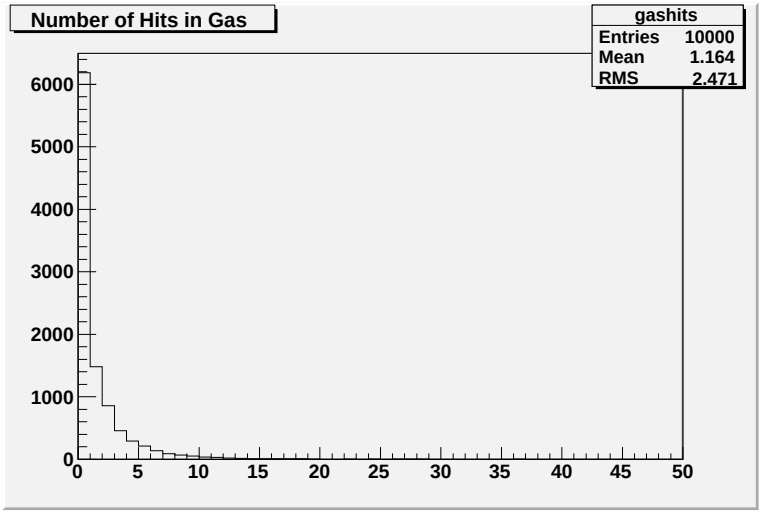

FIG. 33: tape7 th

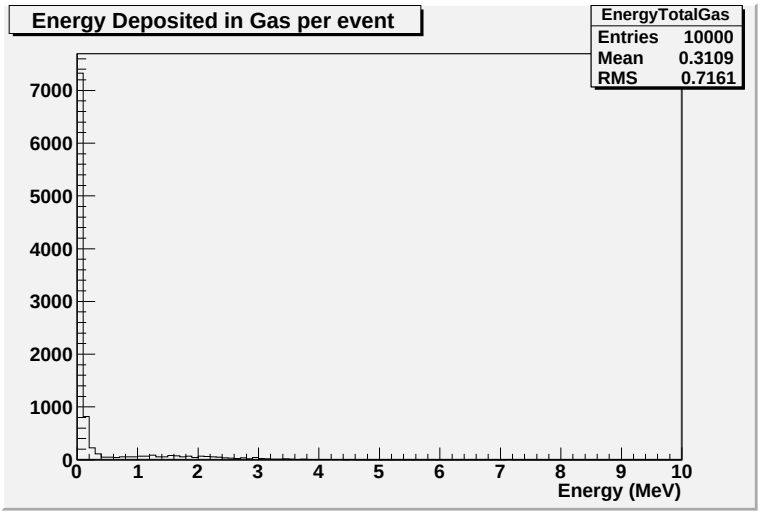

FIG. 34: tape7 th

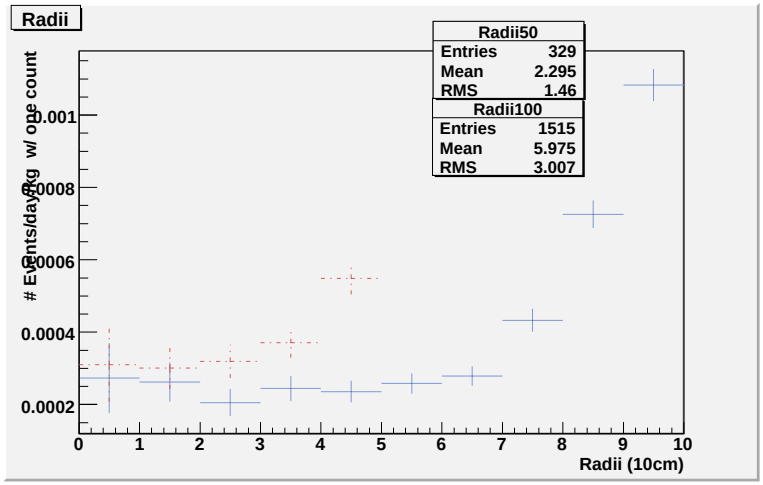

FIG. 35: ss th

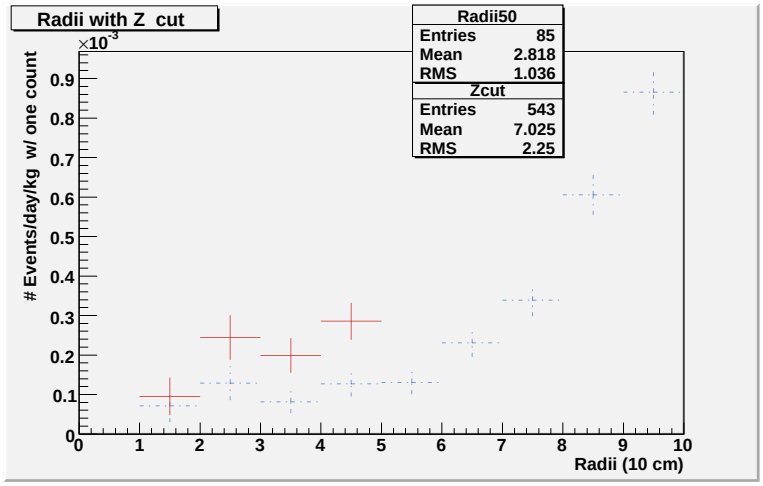

FIG. 36: ss th

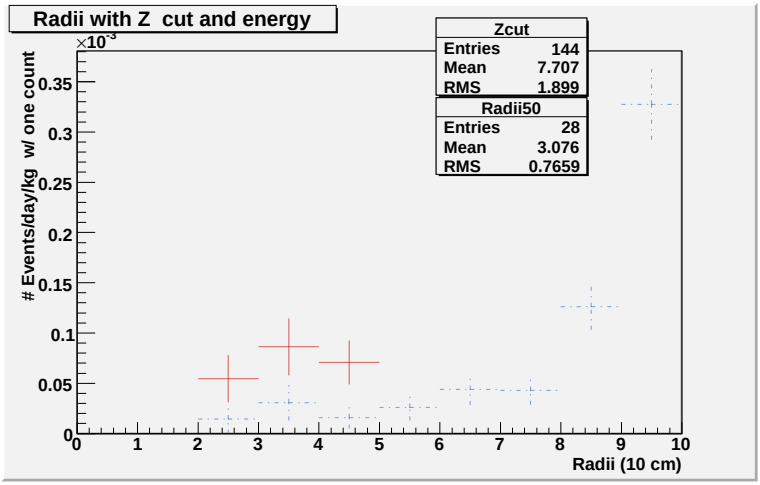

FIG. 37: ss th

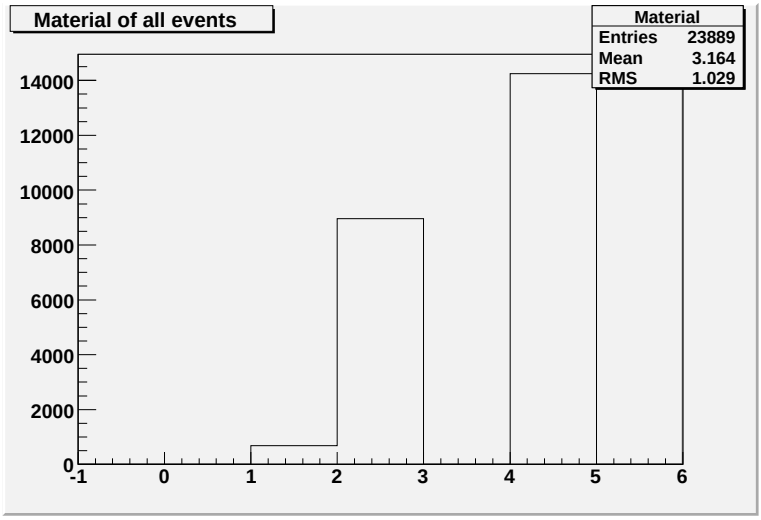

FIG. 38: ss th

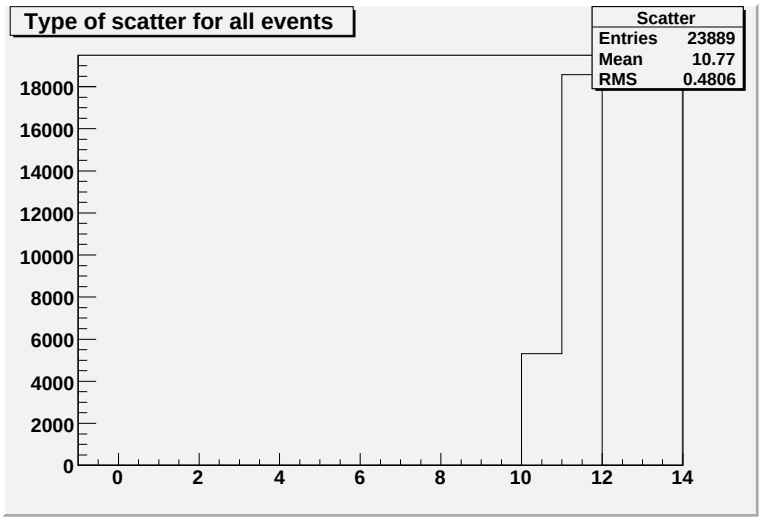

FIG. 39: ss th

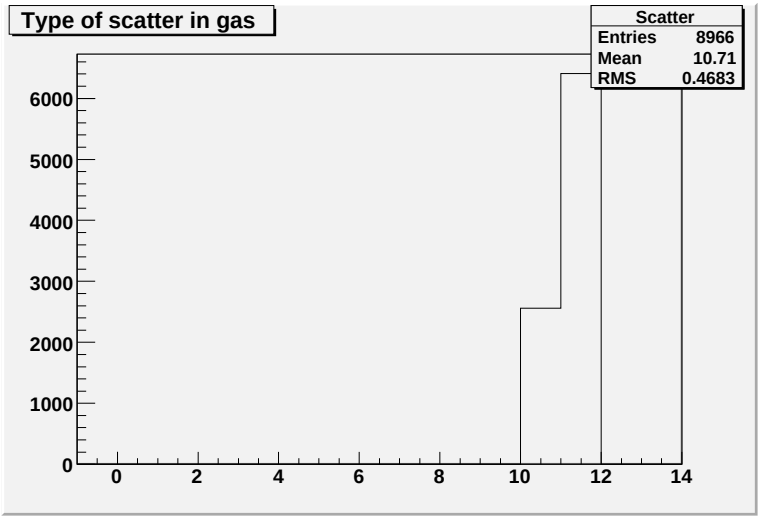

FIG. 40: ss th

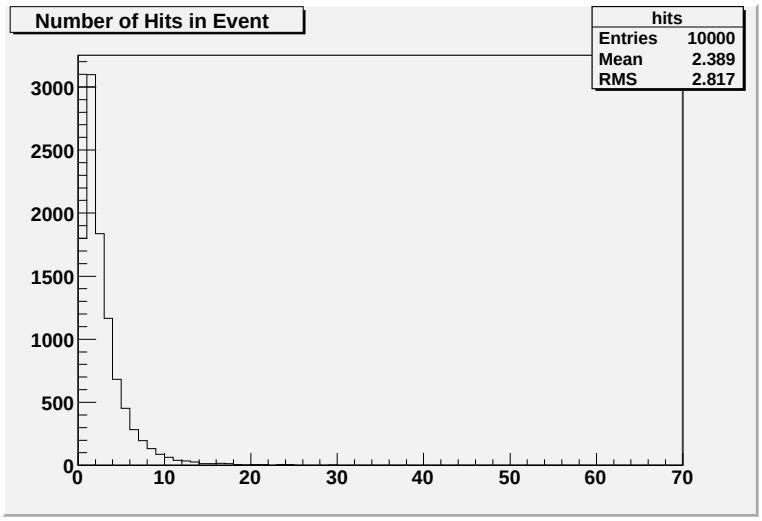

FIG. 41: ss th

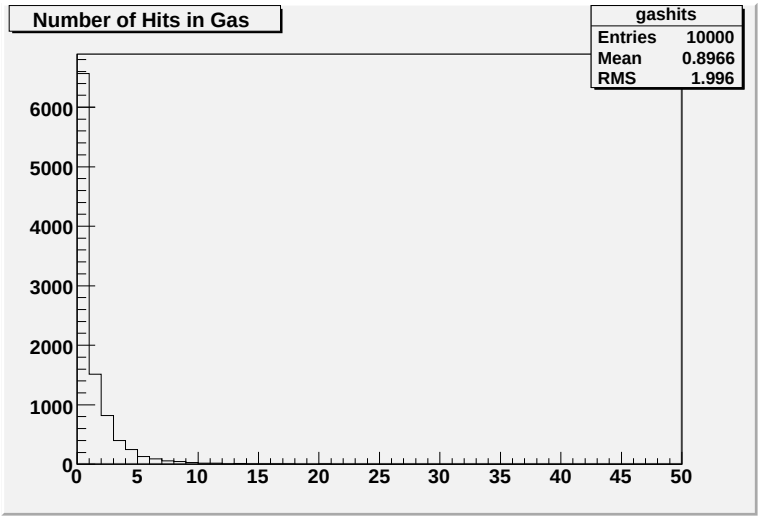

FIG. 42: ss th

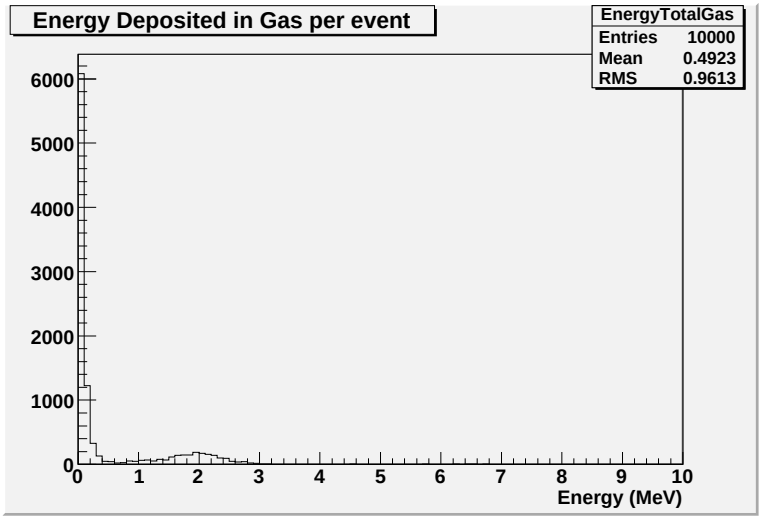

FIG. 43: ss th

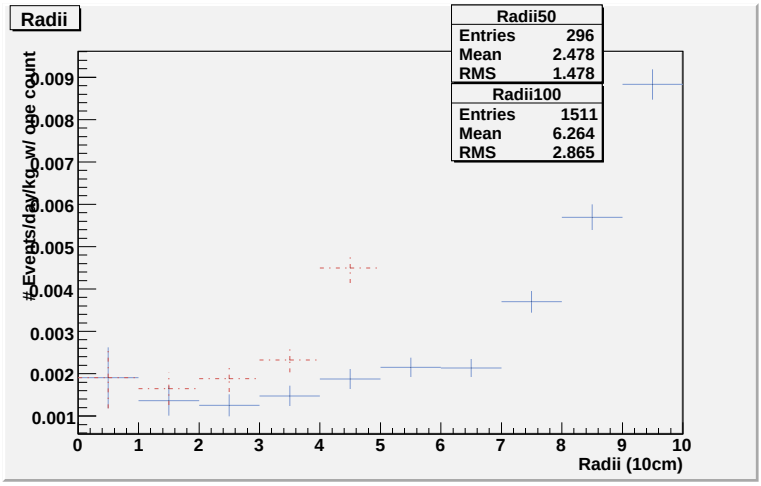

FIG. 44: ss u

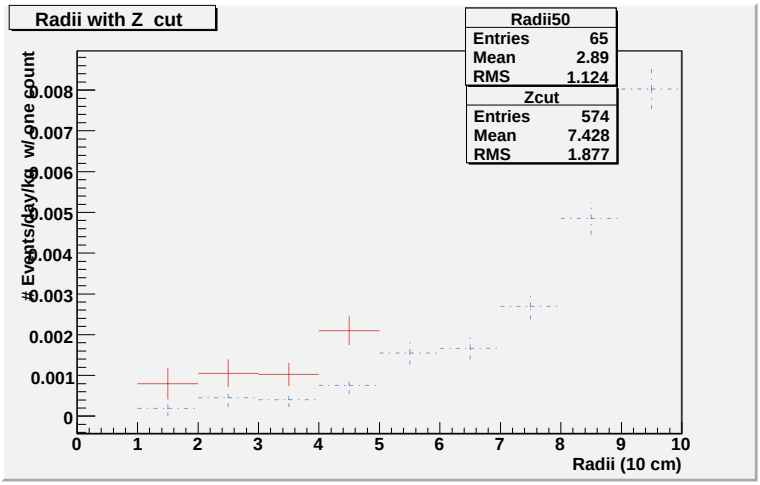

FIG. 45: ss u

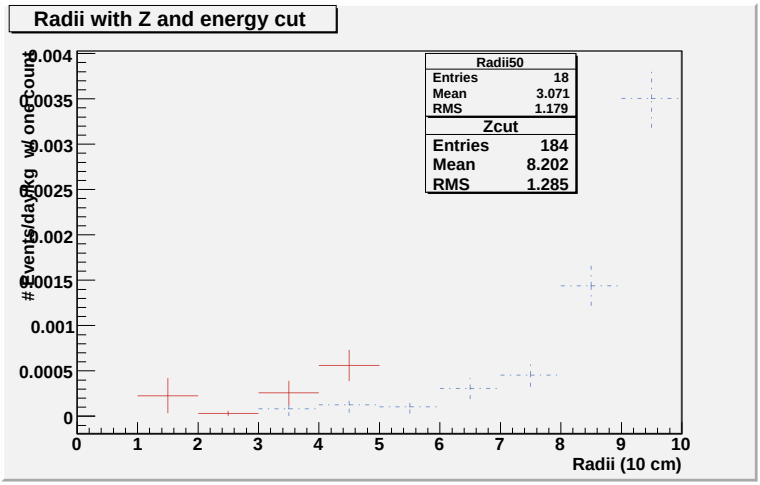

FIG. 46: ss u

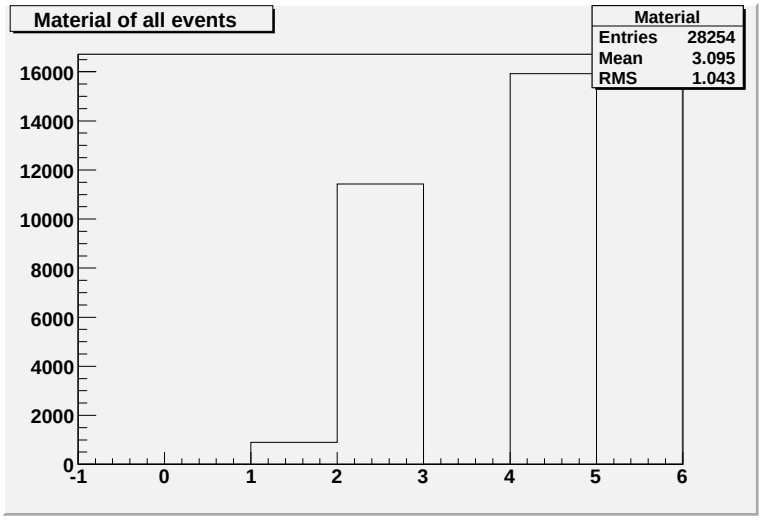

FIG. 47: ss u

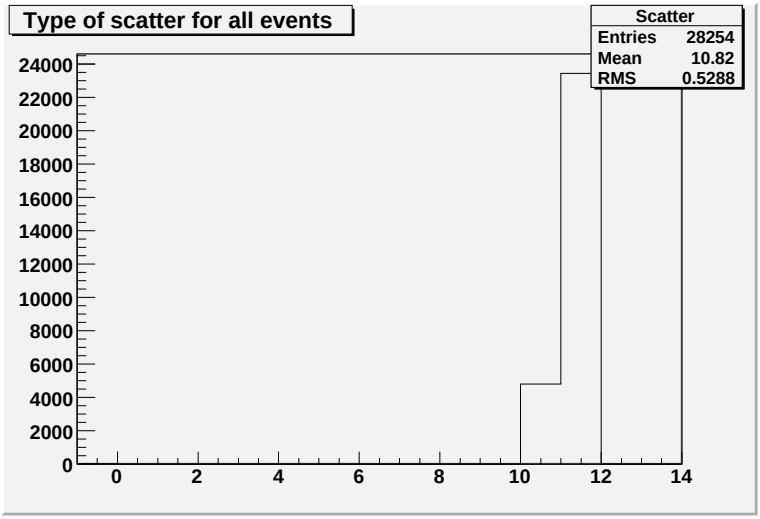

FIG. 48: ss u

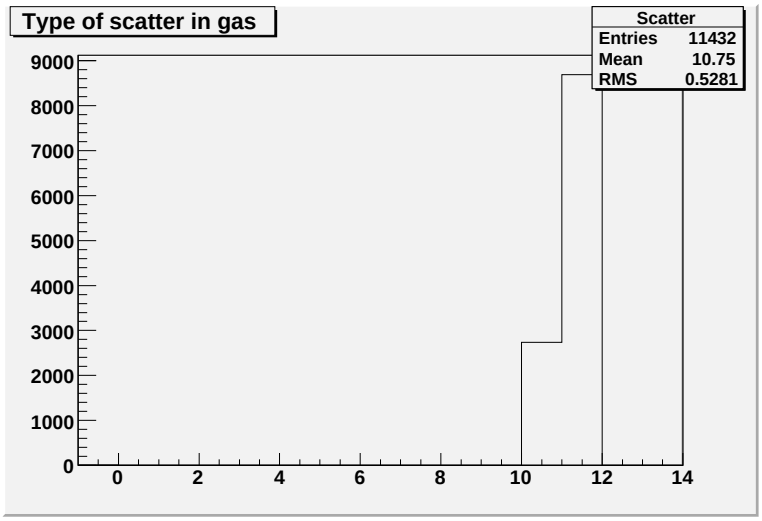

FIG. 49: ss u

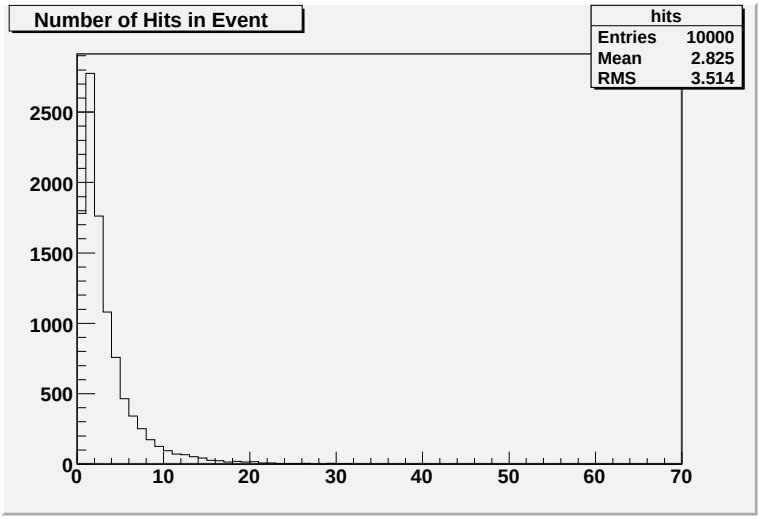

FIG. 50: ss u

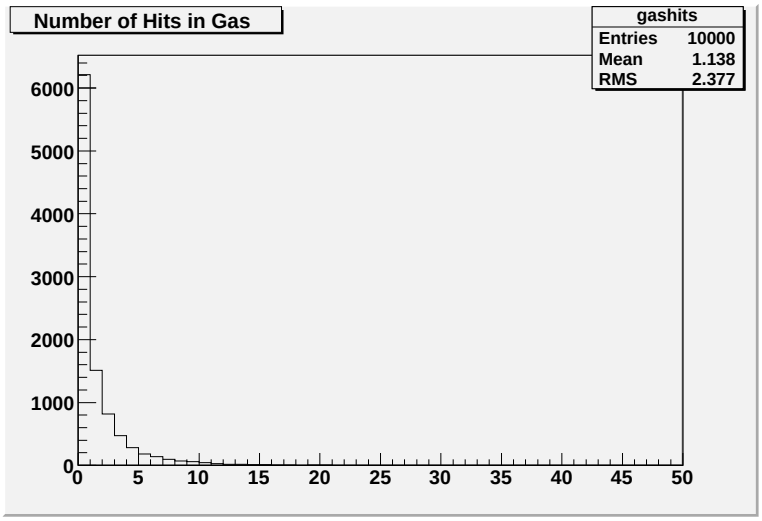

FIG. 51: ss u

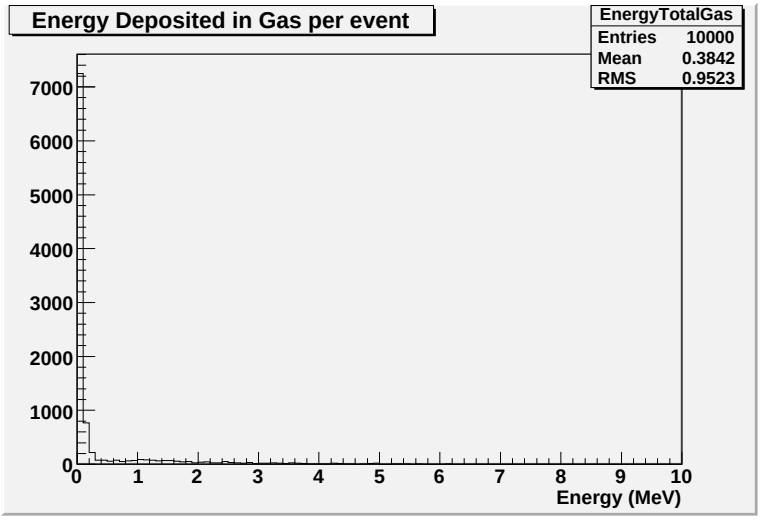

FIG. 52: ss u